

Estimation and modeling of the harmonic drive transmission in the Mitsubishi PA-10 robot arm*

Christopher W. Kennedy and Jaydev P. Desai¹

Program for Robotics, Intelligent Sensing and Mechatronics (PRISM) Laboratory
3141 Chestnut Street, MEM Department, Room 2-115
Drexel University, Philadelphia, PA 19104, USA
Email: {cwk,desai}@coe.drexel.edu

Abstract

The purpose of this paper is to present our results in developing a dynamic model of the Mitsubishi PA-10 robot arm for the purpose of low velocity trajectory tracking using very low feedback gains. The novelty of this research is therefore the development of a systematic algorithm to extract the model parameters of a harmonic drive transmission in the robot arm to facilitate model-based control. We have chosen the elbow pitch joint (joint 4) of the PA-10 robot arm for estimation and modeling purposes. We have done several experiments to identify the various parameters of the harmonic drive system. We conclude with a sample trajectory tracking task whereby the feedback torque required to do trajectory tracking with and without the parameter identification of the HDT is significantly different.

1 Introduction

Accurate modeling of the inherent dynamics of a robot manipulator is essential in many manipulation tasks. Through careful modeling, low feedback gains can be used along with a feedforward model to accurately follow a desired trajectory for tasks requiring low interaction forces while manipulating and interacting with objects in the environment.

The purpose of this paper is to present our results in developing a dynamic model while taking into account the inherent dynamics of the Mitsubishi PA-10 robot arm for the purpose of low velocity trajectory tracking using very low feedback gains. The PA-10 is ideal for precision manipulation tasks due to the backdrivability, precise positioning capabilities and zero backlash afforded by its harmonic drive transmission. However, the compliance and oscillations inherent in harmonic

*This material is based upon the work supported by the National Science Foundation grants EIA 0079830, and CAREER award IIS 0133471 and the American Heart Association grant 0160368U.

¹Corresponding author

drive systems make the development of an accurate dynamic model of the robot extremely challenging. The novelty of this research is therefore the development of a systematic algorithm to extract the model parameters of a harmonic gear driven transmission in the Mitsubishi PA-10 robot arm. This robot is significantly used in research laboratories [1-3] and we believe that this paper is the first of its kind to address the transmission modeling and implementation on the Mitsubishi PA-10 robot arm in a research environment.

There is a substantial body of previous research in the area of modeling harmonic drive systems [4-6]. Tuttle [4] presents an excellent overview of modeling and parameter identification of harmonic drive systems and Kircanski [5] provides a detailed analysis of the nonlinear behavior of harmonic gears due to compliance, friction and hysteresis. Although these research efforts provide significant insight into the physical phenomena that characterize harmonic drive behavior, all of their experimental work has been performed on custom-designed, elaborate test-beds that allow direct measurement of many important system parameters such as compliance and kinematic transmission error. In addition, many control schemes for harmonic drive systems rely on torque sensors mounted directly to the transmission components [7-9]. To our knowledge, there is no published work to date describing an efficient means of modeling, parameter identification, and control of the HDT in the Mitsubishi PA-10 robot arm.

This paper is organized as follows: in section 2, the PA-10 system is described, including the control system architecture, section 3 offers a brief overview of harmonic drive transmissions along with a model of harmonic gearing, section 4 outlines our methods for experimentally determining the necessary parameters for model-based control of the PA-10 robot arm, section 5 details our experiments designed to verify the effectiveness of our model, and finally in section 6 concluding remarks are presented.

2 The Mitsubishi PA-10 Robot

The Mitsubishi PA-10 robot arm is a 7 degree-of-freedom robot arm with an open control architecture and is manufactured by Mitsubishi Heavy Industries (see Figure 1a). The four layer control architecture is made up of the robot arm, servo controller, motion control card, and the upper control computer. The host computer runs the QNX real-time operating system and achieves communication rates of up to 700 Hz with the robot servo driver through the ARCNET motion control card. ARCNET is a token passing LAN protocol developed by Datapoint Corporation.

The robot joints are actuated through three-phase AC servo motors and harmonic drive gear transmissions. Joint positions are measured through resolvers at the joint output axis, with a resolution of 0.000439° over ± 3 output revolutions.

Control of the robot can be achieved in either 'Velocity mode' or 'Torque mode'. In 'Velocity mode', the desired velocity for each joint is sent to the servo driver from the host computer. A high-gain digital PI feedback loop running at 1538 Hz on the servo driver then controls the joint velocity. In 'Torque mode' the desired joint torque (in this case the motor torque constant times the motor current, before conversion by three-phase), is sent to the servo driver. The expression for communicating a desired torque to the robot arm through the servo driver in this system is given by:

$$T_m = k_T * I = T_d * (0.001 \text{ Nm/dig}) \quad (1)$$

where T_m is the motor torque, k_T is the motor torque constant, I is the motor current, and T_d is the desired torque written to the servo driver in the form of a 2 byte integer.

3 Harmonic Drive Systems

Harmonic drive gears, also called strain-wave gearing, were developed by C. Walton Musser in the 1950's primarily for aerospace applications. They are compact, light-weight, and have torque ratios between 30:1 and 320:1, making them ideal for robotics applications. Harmonic drives are composed of three components: the wave generator, the flexspline and the circular spline (see Figure 1). The wave generator is an elliptical ball bearing assembly and is nested inside the flexspline. The teeth on the nonrigid flexspline and

the rigid circular spline are in continuous engagement. Since the flexspline has two teeth fewer than the circular spline, one revolution of the input causes relative motion between the flexspline and the circular spline equal to two teeth. With the circular spline rotationally fixed, the flexspline rotates in the opposite direction to the input at a reduction ratio equal to one-half the number of teeth on the flexspline. The displacement, velocity and torque relationships between the transmission elements in the ideal case are therefore given by:

$$\theta_{wg} = (N + 1)\theta_{cs} - N\theta_{fs} \quad (2)$$

$$\omega_{wg} = (N + 1)\omega_{cs} - N\omega_{fs} \quad (3)$$

$$T_{wg} = \frac{1}{(N + 1)}T_{cs} = \frac{1}{N}T_{fs} \quad (4)$$

where N is the transmission ratio, θ_{wg} is the wave generator angle, θ_{cs} is the circular spline angle, θ_{fs} is the flex spline angle, ω_{wg} is the wave generator angular velocity, ω_{cs} is the circular spline angular velocity, ω_{fs} is the flexspline angular velocity, T_{wg} is the wave generator torque, T_{cs} is the circular spline torque, and T_{fs} is the flexspline torque. In general either the flexspline or the circular spline can be fixed. However, in our robot the circular spline is fixed while the flexspline rotates with the joint.

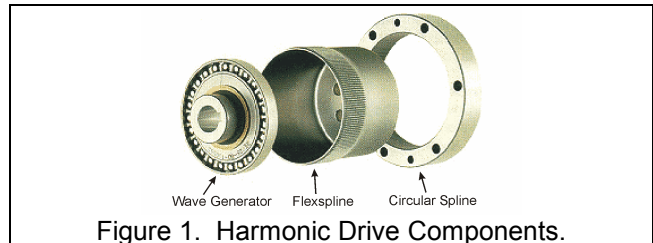


Figure 1. Harmonic Drive Components.

The flexibility inherent in the harmonic drive systems provides advantages such as zero backlash due to natural preloading. However, there are also several disadvantages such as nonlinearity due to friction, alignment error of the components, and transmission losses due to compliance in the system. All of these were found to be critical in the modeling of the Mitsubishi PA-10 robot arm.

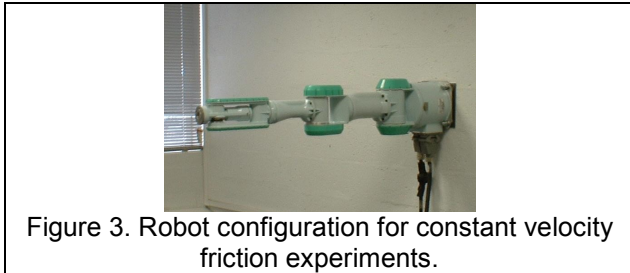
In the following subsections we will describe in detail our methodology for estimation and modeling of the: a) friction in a HDT, b) torsional stiffness, and c) the kinematic transmission error. This will be followed by a model of the HDT for the Mitsubishi PA-10 robot arm.

4 Experimental Methods

We have chosen the elbow pitch joint (joint 4) for analysis because it not only is strongly influenced by gravity and friction, but also is the most affected by the oscillations induced by kinematic error. During normal operation with the high gain controllers, the joint emits a chattering noise due to vibration. This joint will therefore benefit most by accurate modeling. Although we present results for the elbow pitch joint only, we have observed similar behavior in the other joints with the exception of the chattering noise.

4.1 Friction Characterization

Friction is typically characterized by its relationship with velocity. To determine the friction-velocity relationship, the robot was commanded to move at a constant velocity and the mean torque required to maintain the velocity was taken to be the friction for that value of velocity. After collecting data for velocities from 0.005 rad/s to 0.5 rad/s in increments of 0.05 rad/s, the data was fit to the friction model in equation (5). To collect this data, the robot was mounted on the wall as shown in Figure 3 to negate the effect of gravity. The results for the dynamic friction are shown in Figure 4.



To obtain our model of coulomb friction, torque data was collected in 'Velocity mode' to maintain a velocity of 0.005 rad/s. This data was then fed-forward in the form of a look-up table to represent coulomb friction.

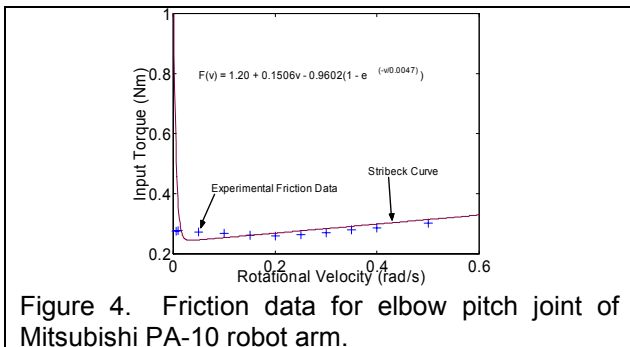


Figure 4. Friction data for elbow pitch joint of Mitsubishi PA-10 robot arm.

4.2 Estimation and modeling of Stiffness, Gravity Compensation, and Kinematic Error

To determine the effect of stiffness and gravity, we commanded the elbow pitch joint to move at a constant velocity of 0.01 rad/s from -90° to $+90^\circ$ with weights from 0 to 10 lbs attached to apply torque to the drive. The output torque required to track this trajectory for weights of 0, 5, and 10 lbs is shown in Figure 5.

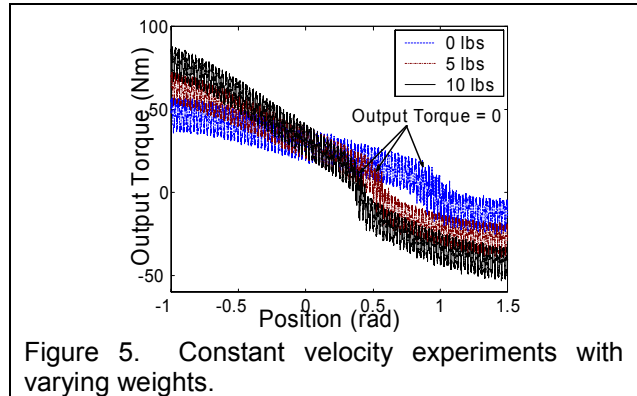


Figure 5. Constant velocity experiments with varying weights.

The effects of gravity and stiffness are clearly evident from these plots. Note the sharp decrease in torque when the output torque approaches 0 Nm. This is due to the 'soft wind-up' behavior of the harmonic drive system. As the load on the wave generator decreases, the stiffness if the wave generator decreases, hence more torque output is required to sustain motion.

We determined the torque used to deform the wave generator during the motion in Figure 5 by equating the output torque during the motion with the right side of equation (7). The friction torque for these motions is nearly identical to the coulomb friction, hence we can eliminate friction from equation (7) by subtracting the coulomb friction torque from the total torque (as noted previously, coulomb friction torque was computed from the arm motion at low velocity while it was attached to the wall). The gravity torque is also known from the estimated masses of the robot arm links and the known weights attached to the robot. We can therefore subtract the gravity torque from the right side of equation (7). This leaves the remaining torque equal to the torque used to deform the wave generator. The successive plots of each step of this process are shown in Figure 6.

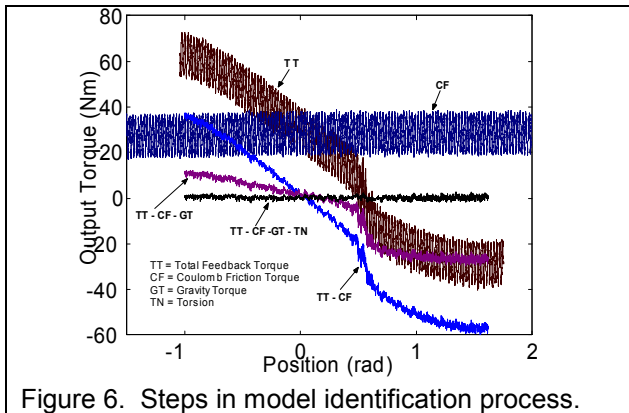


Figure 6. Steps in model identification process.

To verify that this approach is valid, the stiffness torque calculated as described above was plotted as a function of the external torque (gravity plus mean coulomb friction) for each of the three weight trials in both the positive and negative directions (Figure 7).

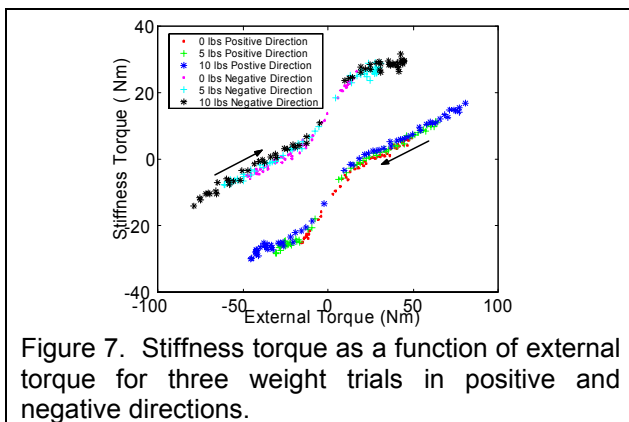


Figure 7. Stiffness torque as a function of external torque for three weight trials in positive and negative directions.

As can be observed from Figure 7, the model of stiffness torque as a function of external load appears to be fairly repeatable. The region where the torque decreases or increases sharply due to a rapidly changing stiffness coefficient seems to be modeled effectively. We model this function as composed of three linear regions for each direction.

For the feedforward implementation, we use the data collected in the previous experiments to generate a relationship between the external load and the input torque required to generate the necessary output torque to compensate for the load.

5 Results

To verify our model, we fed forward the computed torques to track a trapezoidal velocity profile at 0.1 rad/s. The gains were set to 0.5 N and 0.15 Ns for

the proportional and derivative gains respectively. Velocity measurements were taken by differentiating the position measurements and filtered using a fifth order Butterworth filter with a cutoff frequency of 200 Hz. This filter was chosen because it was empirically determined to give the best results. The feedback torques generated while tracking the desired trajectory are shown in Figure 8 for the low gain implementation with the feedforward model, and for the high gain implementation with no feedforward model. The magnitude of the feedback torques is approximately 1 Nm in the region of high wave generator stiffness and approximately 6 Nm in the region of low wave generator stiffness for the low gain feedforward case.

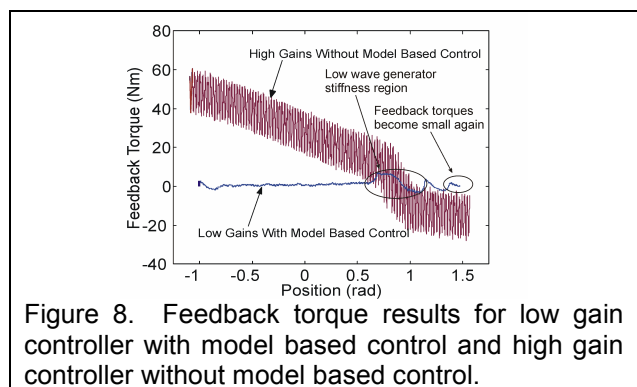


Figure 8. Feedback torque results for low gain controller with model based control and high gain controller without model based control.

The tracking error for the low gain feedforward case is shown in Figure 9. The mean tracking error is approximately 0.02 radians in the region of high wave generator stiffness, and 0.2 radians in the region of low wave generator stiffness.

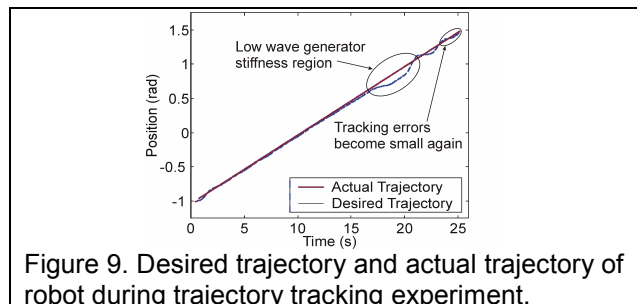


Figure 9. Desired trajectory and actual trajectory of robot during trajectory tracking experiment.

5 Discussion

Our approach in developing a dynamic model for the HDT in the Mitsubishi PA-10 robot arm can be described as follows: 1) we developed a mathematical model for the HDT accounting for friction, transmission compliance and gravity, resulting in equation (6), 2) we characterized friction in the transmission using constant velocity experiments, 3) we commanded the robot to move

along a test trajectory with weights of known magnitude attached to determine the effect of transmission compliance, and 4) we determined the model parameters based on the experimental data and then fed forward our model to the robot for the purpose of tracking a desired trajectory.

As shown in Figure 7, there are separate curves for the stiffness torque when the experiment is performed in the positive and negative directions. Recall that our definition of coulomb friction is the torque required to maintain a very slow velocity of the range of motion of the joint. Therefore, the effect of wave generator deformation has already been taken into account in our friction model for a given direction. Because the non-linear stiffness behavior of the wave generator occurs only in a narrow region of low applied torques (lower than the torque required to initiate motion), its effect is not noticeable at higher applied loads.

If our model is accurate, very low feedback gains can be used to track a given trajectory. The results of the feedforward implementation are shown in Figures 8 and 9. As observed from the plots, the model performs very well for external loads not within the region of low wave generator stiffness, as evidenced by the low feedback torques and tracking errors. However, within the region of low wave generator stiffness, there is an increase in feedback torque and tracking error. After the robot passes through the region of low wave generator stiffness, the feedback torques and tracking errors again become very small. One possible reason for this increase in error is the abrupt change in the wave generator stiffness. Very small errors in modeling where this change in wave generator stiffness occurs could generate large errors in the calculated torques required to track the trajectory accurately.

6 Conclusion

We have presented our initial results in developing a dynamic model of the harmonic drive transmission in the Mitsubishi PA-10 robot arm for the purpose of low velocity trajectory tracking using very low feedback gains. A model of the HDT in one joint of the robot was developed that successfully allowed low velocity trajectory tracking outside the region of low wave generator stiffness for joint 4. We have chosen the elbow pitch joint (joint 4) for analysis because it not only is strongly influenced by gravity and friction, but also is the most affected by the oscillations induced by kinematic error. The Mitsubishi PA-10 is widely used in research laboratories, yet no published

work addresses the modeling of the dynamical properties of the HDT. We believe that this work is therefore essential for effective model-based control of the Mitsubishi PA-10 robot arm and wider dissemination to the research community. In the future, our work will focus on refining our model in the region of low wave generator stiffness and implementing a complete model based control for our robot including all of the robot's joints.

References

1. Hirata, Y., et al. *Manipulation of a large object by multiple DR helpers in cooperation with a human*. in *International Conference on Intelligent Robots and Systems*. 2001.
2. Yoon, W.K., Y. Tsumaki, and M. Uchiyama. *An experimental system for dual-arm robot teleoperation in space with concepts of virtual grip and ball*. in *International Conference on Advanced Robotics*. 1999. Tokyo, Japan.
3. Olsen, M.M. and H.G. Peterson, *A New Method for Estimating Parameters of a Dynamic Robot Model*. *IEEE Transactions on Robotics and Automation*, 2001. **17**(1): p. 95-100.
4. Tuttle, T.D., *Understanding and modeling the behavior of a harmonic drive gear transmission*. 1992, Masters Thesis, MIT Artificial Intelligence Laboratory.
5. Kircanski, N. and A.A. Goldenberg, *An experimental study of nonlinear stiffness, hysteresis, and friction effects in robot joints with harmonic drives and torque sensors*. *International Journal of Robotics Research*, 1997. **16**(2): p. 214-239.
6. Taghirad, H.D., *On the modeling and identification of harmonic drive systems*. 1997, Centre for Intelligent Machines, McGill University.
7. Godler, I., T. Ninomiya, and M. Horiuchi, *Ripple compensation for torque sensors built into harmonic drives*. *IEEE Transactions on Instrumentation and Measurement*, 2001. **50**(1): p. 117-122.
8. Hashimoto, M., et al. *Experimental study on torque control using harmonic drive built-in torque sensors*. in *IEEE International Conference on Robotics and Automation*. 1992. Nice, France.
9. Taghirad, H.D. and P.R. Belanger, *Torque ripple and misalignment torque compensation for the built-in torque sensor of harmonic drive systems*. *IEEE Transactions on Instrumentation and Measurement*, 1998. **47**(1): p. 309-315.